Springer

KSME

Journal of Mechanical Science and Technology 24 (4) (2010) 977~982
www.springerlink.com/content/1738-494x
DOI 10.1007/s12206-010-0210-1

Structure analysis of bubble driven flow by time-resolved PIV and POD techniques †

Hyun Dong Kim[1], Seung Jae Yi[1], Jong Wook Kim[1] and Kyung Chun Kim[2,*]

[1]*Department of Mechanical Engineering, Pusan National University, Busan, 609-735, Korea*
[2]*School of Mechanical Engineering, Pusan National University, Busan, 609-735, Korea*

(Manuscript Received July 20, 2009; Revised October 27, 2009; Accepted December 12, 2009)

Abstract

In this paper, the recirculation flow motion and turbulence characteristics of liquid flow driven by air bubble stream in a rectangular water tank are studied. The time-resolved Particle Image Velocimetry (PIV) technique is adopted for the quantitative visualization and analysis. 532nm Diode CW laser is used for illumination and orange fluorescent (λ_{ex} = 540nm, λ_{em} = 584nm) particle images are acquired by a 1280×1024 high-speed camera. To obtain clean particle images, 545nm long pass optical filter and an image intensifier are employed and the flow rate of compressed air is 3ℓ/min at 0.5MPa. The recirculation and mixing flow field is further investigated by time-resolved Proper Orthogonal Decomposition (POD) analysis technique. It is observed that the large scale recirculation resulting from the interaction between rising bubble stream and side wall is the most dominant flow structure and there are small scale vortical structures moving along with the large scale recirculation flow. It is also verified that the sum of 20 modes of velocity field has about 67.4% of total turbulent energy.

Keywords: Bubble driven flow; Time-resolved particle image velocimetry; Proper orthogonal decomposition; Recirculation flow

1. Introduction

Knowledge of bubbly flows is significant to various engineering systems such as nuclear waste treatment, bio-chemical reactors and steel making plants. Especially in the chemical engineering and industrial field, the mixing problems such as powder dispersion, solid blending, and gas dispersion into liquid have been an important issue because of the resulting product quality and productivity are highly depend on the mixing process [1-3]. In turbulent bubbly flow studies, there are two main interests: turbulence modification by bubbles and turbulent mixing due to bubble driven liquid flows.

Previous studies of turbulence modification have shown that dispersed bubbles can either augment or attenuate the liquid phase turbulent kinetic energy [4, 5]. Fujiwara et al. conducted the experimental investigation of vertical pipe flow injected with dispersed bubbles using PIV/LIF, and projecting shadow image technique [6]. They found that the high concentration of bubbles in the vicinity of the wall induces a reduction of the fluctuation velocity intensity of the liquid. However, the external force affected by bubbles is expected to contribute the turbulence energy production.

To enhance mixing efficiency for a bubble-driven mixer such as high temperature mixing condition, air bubbling can be used. In such a system, gas is injected into a liquid bath from an orifice located at the bottom wall of a liquid container. Durst et al. [7] performed experimental studies on bubble-driven laminar flows by investigating liquid circulation and bubble's street with Laser-Doppler system. It was reported that the liquid-phase circulation pattern is not sensitive to the actual shape of the void fraction profiles. Johansen et al. [8] studied the fluid dynamics in bubble-stirred ladles by employing a Laser-Doppler system to measure the axial and radial mean and fluctuating velocities of liquid phase. Air was supplied through a porous plug placed in the bottom wall of a cylindrical perspex-water model of a ladle. Very recently, Montante et al. [9] measured the turbulent gas-liquid flow and bubble size distribution in aerated stirred tanks using a two-phase PIV and a digital image processing method based on a threshold criterion. However, their experiments were not a pure bubble-induced flow but a Rushton turbine is included in the mixing tank.

Due to the lack of detailed experimental data in the bubble-driven mixing flow in the rectangular tank, it is needed to provide accurate velocity field data with appropriate time and space resolution. Since the mixing characteristics in the bub-

† This paper was recommended for publication in revised form by Associate Editor Kyung-Soo Yang
*Corresponding author. Tel.: +82 51 510 2324, Fax.: +82 51 515 7866
E-mail address: kckim@pusan.ac.kr

ble-driven turbulent liquid flows is dominantly governed by the large scale motions in the flow field, the analysis of the large scale dynamics is necessary to understand the mixing mechanism. In this study, we aimed to measure the entire flow and analysis the large scale dynamic structures and turbulent characteristics in the bubble-driven liquid flow in a rectangular tank by using the time-resolved PIV and POD techniques for the bubbling mixer.

2. Experimental setup

In this study, a typical 2-dimensional time-resolved PIV system is adopted as shown in Fig. 1. The tank size is 300 × 300 × 300 mm^3 and a rectangular shape. To understand dynamic flow structures based on the time-resolved PIV technique, accurate quantitative visualization should be required. For that reason, the rectangular tank was selected as a mixing vessel to acquire more clear and undistorted images. Tap water is filled with 150 mm height. The nozzle is located on the bottom of the tank, and the diameter of nozzle is 20mm (D_N=20mm). The orange fluorescent particle (D_p=10μm, λ_{ex}=540nm, λ_{em}=584nm) is used to reduce the diffused reflections because of the edge of bubble and tank. A PCO 10bit high speed CCD camera (1280 × 1024) is used for orange fluorescent particle imaging and a laser sheet beam of 2mm thickness created by a spherical lens and cylindrical lens was irradiated to the object plane from 532nm Diode CW laser for illumination. The 545nm long pass optical filter and an image intensifier are employed to get clean particle images. Time interval between each image is 12.5ms (80 frames per second) Since the highest frequency of the periodical generation of air bubble is about 10Hz, 80 frames per second mode with 1280 × 1024 pixels spatial resolution is chosen to satisfy the Nyquist sampling frequency. The images are interrogated by the two-frame cross-correlation technique. Interrogation windows are taken to be 64 × 64 pixels, respectively, the FFT window size is set to 48 × 48, and a 50% overlap was used. Final vector fields were acquired through the interrogation by the PIV-Sleuth program. The field-of-view size is 100 mm × 90 mm and measurement (laser sheet) position is the left side of bubbler. Tab water was used as a working fluid and compressed air is used for formation of bubble stream. Air flow rate is 3 ℓ /min at 0.5MPa

Fig. 2 describes coordinate system adopted in this study and position of field of view. The origin of coordinate system is decided to the center of bubbling nozzle. The height of X-axis is 20mm from the bottom and Y-axis is aligned to center of nozzle. Right end line of field of view is 40mm apart from the Y-axis and bottom end is aligned to X-axis.

3. Proper orthogonal decomposition

Dynamic information of the flow field can be explained effectively by POD (Proper Orthogonal Decomposition), from which the relative energy distribution is acquired. By using the

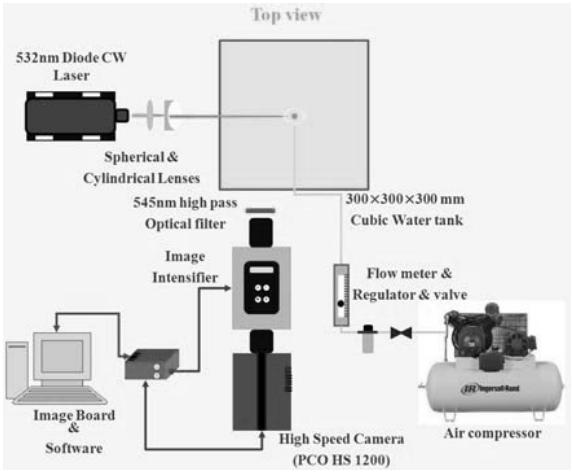

Fig. 1. Experimental setup for time resolved PIV measurement in a bubbling tank.

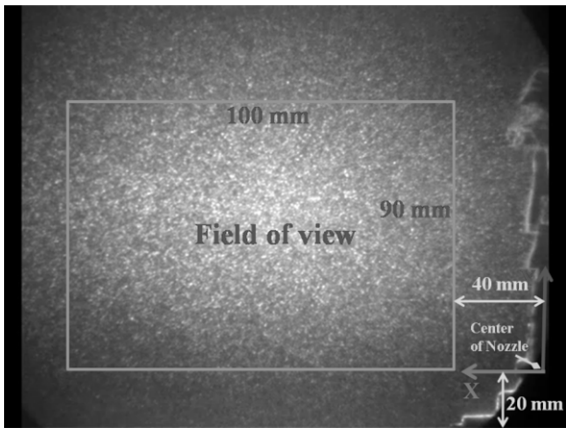

Fig. 2. Coordinate system and position of field of view for the PIV measurement.

POD technique as proposed by Lumley, The flow field can be decomposed into optimal orthogonal spatial modes and optimal orthogonal temporal modes:

$$\mathrm{u}(\mathrm{x},t)=\sum_{\mathrm{n}} a^{(n)}(t)\varphi^{(n)}(\mathrm{x}) \tag{1}$$

The optimality means that POD minimizes the mean square error of any partial sum of expansion and conversely the expansion in terms of these bases obtained by POD converges faster than the expansion in terms of any other basis such as Fourier decomposition. The spatial modes $\varphi^{(n)}(\mathrm{x})$ can be obtained by solving the following integral equation:

$$\int R(\mathrm{x},\mathrm{x}')\varphi^{(n)}(\mathrm{x}')d\mathrm{x}=\lambda^{(n)}\varphi^{(n)}(\mathrm{x}) \tag{2}$$

where λ is the eigenvalue, and $R(\mathrm{x},\mathrm{x}')$ is ensemble-averaged two point correlation function, $\langle u(\mathrm{x})u(\mathrm{x}')\rangle$. The orthogonality of spatial basis and temporal basis is represented as followings as:

$$(\varphi^{(n)}(\mathrm{x}), \varphi^{(m)}(\mathrm{x}')) = \delta_{nm}, \langle a^{(n)}(t) a^{(m)}(t) \rangle = \lambda^{(n)} \delta_{nm} \quad (3)$$

The traditional direct method requires huge calculations, so it takes much time, but Sirovich [10] suggested the method of snapshot that can save calculation time. In this research, in order to find the dynamic structures, we executed a POD analysis using the method of snapshots and the instantaneous fluctuating velocity field:

$$\mathrm{u}(\mathrm{x}, t) = \overline{\mathrm{u}}(\mathrm{x}) + \mathrm{u}'(\mathrm{x}, t) = \overline{\mathrm{u}}(\mathrm{x}) + \sum_{m=1}^{M} \mathrm{a}^{(m)}(t) \varphi^{(m)}(\mathrm{x}) \quad (4)$$

From the calculated eigenmodes, we extracted the turbulent kinetic energy contribution, and compared it with a large-scale structure using the sum of first few modes.

4. Results and discussion

Fig. 3 shows a snapshot of bubble-driven flow visualization. Bubbles move vertically with unsteady mode and arriving to the free surface. From the images of the developed bubbles, mean diameter is estimated as 27 mm and the rising velocity of the bubble is estimated as 0.4 m/s. Based on the rising velocity and the diameter of bubbles, the Reynolds number of the bubble-driven flow is about 7,140 and it confirms that the flow is in turbulent regime. Since the air bubbles are disappeared at the free surface, there is no gas phase in the measurement volume. It should be noted that the buoyancy driven kinetic energy of the bubble generates radial velocity of liquid flow as well as gravitational waves in the free surface which contributes nothing to the flow mixing.

Fig. 4 presents the time-mean velocity field and vorticity contour obtained in the liquid flow driven by the single bubble stream. The definition of vorticity is the curl of the velocity field. The vorticity of two dimensional velocity field is defined as:

$$\omega_z = \frac{\partial v}{\partial x} - \frac{\partial u}{\partial y} \quad (5)$$

The derivatives in Equations are calculated by using 1st order finite difference scheme of partial derivate. The 1st order central difference scheme is used in the region except boundary and 1st order central difference scheme, 1st order forward difference scheme and 1st order backward difference scheme are used at the boundary. A total of 1,750 instantaneous velocity vector fields are used to obtain the mean velocity field. It can be seen that the vertical velocity of liquid entrained to the bubble column is about 0.2 m/s which is about half of the rising velocity. A counter-clockwise circulation is shown in the left side of the water tank from the nozzle.

The center of the vortex is located at the lower left side ($X/D_n = 5.7$, $Y/D_n = 2.1$). Due to the presence of side wall of the tank, radial velocity at the free surface converts to the

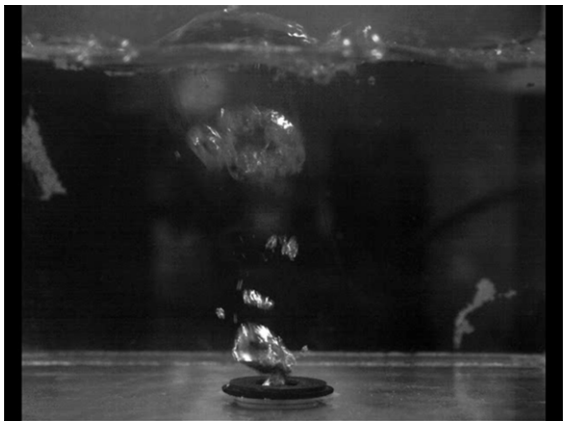

Fig. 3. Visualization of bubble stream and free surface fluctuation in a mixing tank.

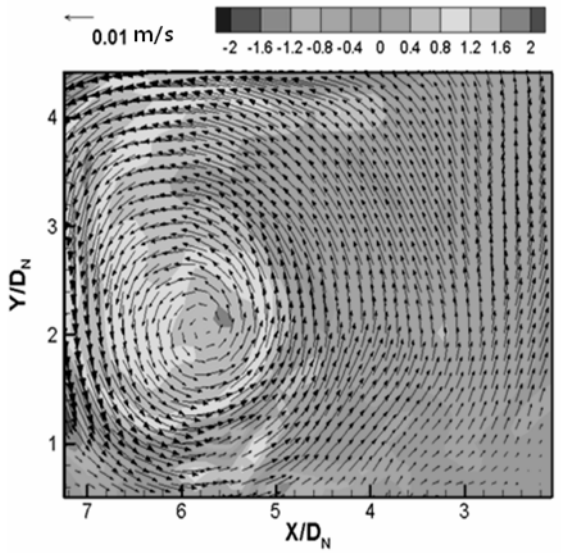

Fig. 4. Ensemble averaged velocity field and vorticity contour.

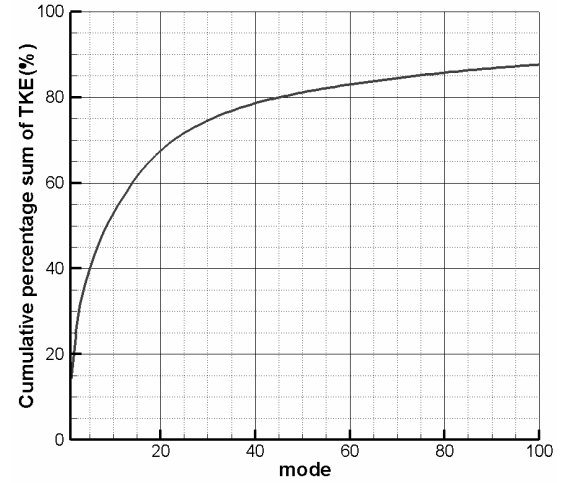

Fig. 5. Cumulative percentage sum of turbulent kinetic energy distribution of first 100 modes.

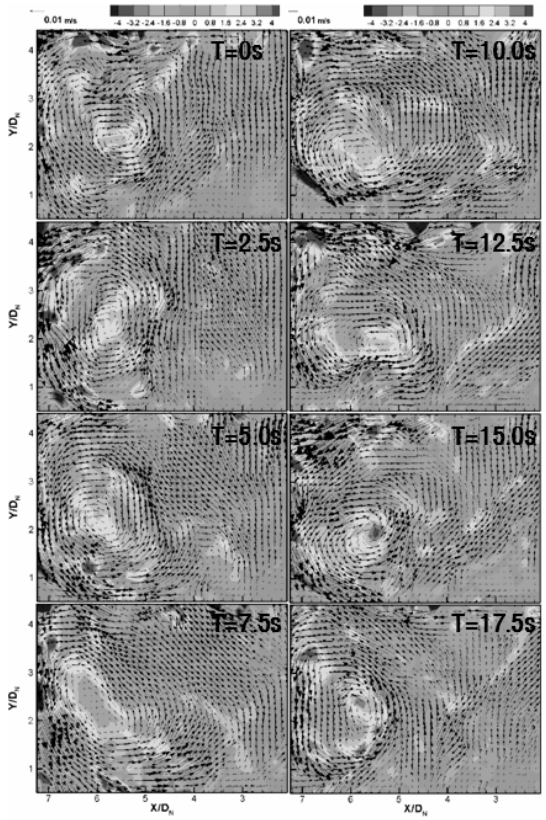

Fig. 6. Time history of instantaneous velocity field and vorticity contour.

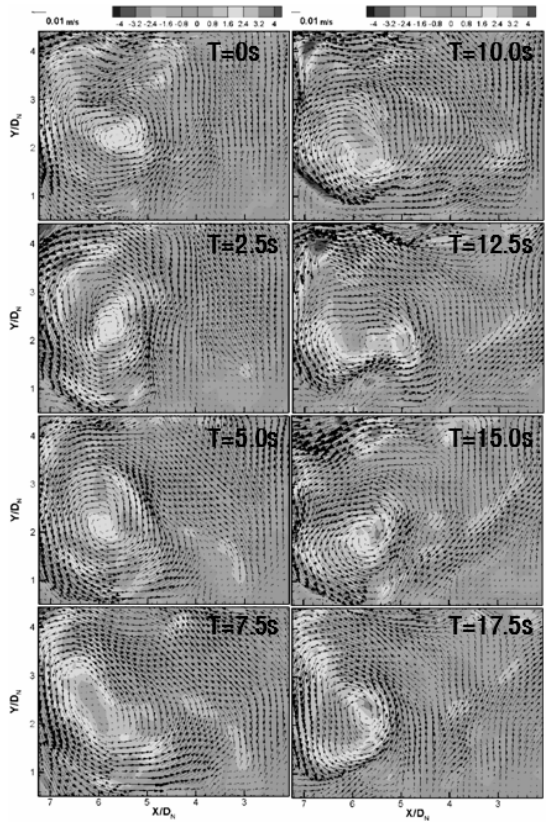

Fig. 7. Reconstructed velocity field with first 20 modes.

downward vertical velocity along the side wall. The penetration of the downward flow reaches very closely to the bottom wall (Y/D_N = 0.3). This means the bubble-induced flow is effective for mixing in the current conditions. The peak value of mean vorticity is located near the vortex core. Negative value of vorticity is observed in the corner region of the tank.

In POD analysis of this study, the eigenvalue represent the turbulent kinetic energy of each mode. Fig. 5 demonstrates the turbulent kinetic energy distribution and the corresponding cumulative energy sum with respect to the mode number. The time-mean flow field has about 75% of total kinetic energy, which is the dominant dynamic structure in the set of instantaneous velocity fields. It is shown that most of turbulent kinetic energy concentrate on the first few modes and the first 20 modes has about 67.4% of total turbulent kinetic energy in the total velocity fields, which is 91.9% of total kinetic energy if the energy of the time-mean velocity is included.

Fig. 6 depicts the time history of instantaneous velocity fields. It can be seen that the vortex core moves around the time averaged vortex core and the unsteady nature of the strong radial velocity vectors generated by bubbles is clearly observed. Vorticity contour illustrates that the small scale eddies are moving with the main stream of the dominant circulation. The flow field is inherently three dimensional, so that counter rotating vortex pair can be seen in the measurement plane.

Comparison of the instantaneous flow fields measured by PIV and the corresponding reconstructed field from first 20 modes is shown in Fig. 7. As time varies, the deformation of the vortical structure and the movement of the center of vortices are found in Fig. 7. The reconstructed field with the first few modes is obtained by summing time-mean velocity field and the partial sum of eigenmode expansions, which consists of the optimal spatial modes and the optimal temporal modes as shown as Eq. (4). The reconstructed field with the first 20 modes is a low pass filtered velocity field of the instantaneous velocity for passing only the first 20 eigenmodes as compared with the Fig. 6. This result demonstrates that the large scale motions are dominated in the turbulent liquid flow and those motions may govern mixing characteristics in the bubbling mixer.

Fig. 8 represents the spatial modal fields and time histories of temporal modes from 1st to 5th mode. The small oscillations of temporal modes are shown at the time histories, which are caused by the generation of bubble stream. The frequency of the oscillation is similar to the bubble generating frequency, and the value of which is about 4Hz. In the case of the lowest eigenvalue, the corresponding spatial mode represents the most dominant flow structure.

Other, higher spatial modes represent smaller-kinetic-energy and smaller-scale flow structures; that is, of all the flow structures, they represent the high-frequency, small-scale flow structures. The 1st mode (Fig. 8(a)) contains the greatest

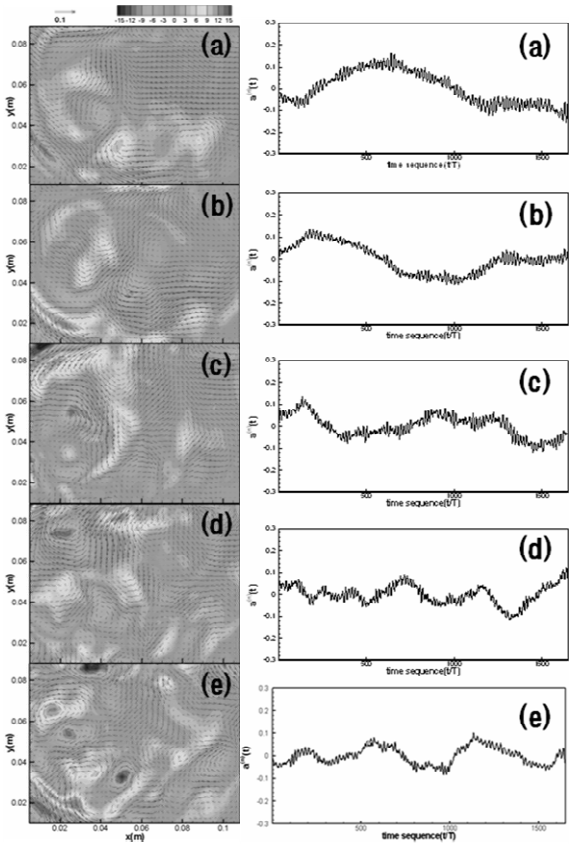

Fig. 8. Spatial modal fields and time histories of temporal modes from 1st to 5th mode; (a)1st mode, (b)2nd mode, (c)3rd mode, (d)4th mode, (e)5th mode.

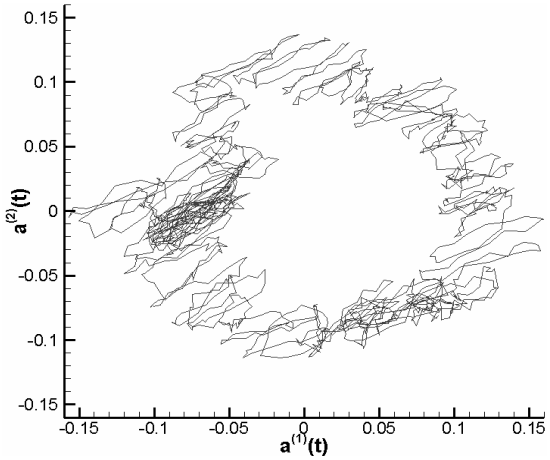

Fig. 9. Phase space projection of 1st temporal mode and 2nd temporal mode.

quantity of turbulent energy. We recognized that two counter-rotating vortices are inside the recirculating zone of the mean flow and large momentum region around the recirculating zone. The 2nd spatial mode (Fig. 8(b)) has three vortical structures related to the mean recirculating flow. Two vertically-aligned counter-rotating vortices and a strong vortex induced the fluid to the bottom wall of that four counter-rotating vortices aligned with the high turbulent kinetic energy region and the 4th spatial mode has eight smaller vortices along the edge of the mean recirculating zone. The 3rd and 4th temporal modes have the same frequency and phase, but the frequency is twice that of the modes shown in Figs. 6(a) and (b).

Fig. 9 represents the phase-space projection of the 1st temporal mode and the 2nd temporal mode. It is shown that the projection has approximately circular shape with small oscillation along the circular shape. This means the 1st and 2nd modes have the same frequency and out of phase relation. The phase-space projection shows the periodic nature in small and large time scales. Kim et al. [11] found the similar unsteady nature of sinusoidal oscillation in the impinging jet flow to the confined wall.

5. Conclusion

To investigate the characteristics of the bubble-driven flow, the time-resolved PIV techniques are adopted for the quantitative visualization and analysis. The measured flow field is investigated by time-resolved POD technique. From the calculated spatio-temporal modes obtained by POD analysis, we extracted the turbulent kinetic energy contribution and the corresponding dynamic structures. The 1st and 2nd spatio-temporal modes are found to influence on the deformation of the dominant vortical structure.

Acknowledgment

This work was supported by the Korea Science and Engineering Foundation (KOSEF) grant funded by the Korea government (MEST) (No. 2009-0080535). The first three authors were supported by the second phase of the Brain Korea 21 Program in 2009.

References

[1] W. Luewisutthichat, A. Tsutsumi and K. Yoshida, Chaotic Hydrodynamics of Continuous Single-Bubble Flow Systems, *Chemical Engineering Science*, 52 (1997) 3685-3691.

[2] P. Tirto, T. Koichi and T. Hideki, Effect of Operating Conditions on Two-Phase Bubble Formation Behavior at Single Nozzle Submerged in Water, *Journal of Chemical Engineering*, 34 (2) (2001) 114-120.

[3] X. Tu and C. Trägårdh, Methodology development for the analysis of velocity particle image velocimetry images of turbulent, bubbly gas-liquid flows, *Measurement science & technology*, 13 (7) (2002) 1079-1086.

[4] T. G. Theofanous and J. Sullivan, Turbulence in Two-phase Dispersed Flows, *Journal of Fluid Mechanics*, 116 (1982) 343-362.

[5] S. K. Wang, S. J. Lee, O. C. Jones and R. T. Lahey, Turbulence Structure and Phase Distribution Measurements in Bubbly Two-phase Flows, *International Journal of Multiphase Flow,* 13 (1987) 327-343.

[6] A. Fujiwara, D. Minato and K. Hishida, Effect of Bubble Diameter on Modification of Turbulence in an Upward Pipe Flow, *International Journal of Heat and Fluid Flow*, 25 (2004) 481-488.
[7] F. Durst, A. M. K. P. Taylor and J. H. Whitelaw, Experimental 3and Numerical Investigation of Bubble-driven Laminar Flow in an Axisymmetric Vessel, *International Journal of Multiphase Flow*, 10 (1984) 557-569.
[8] S. T. Johansen, D. G. C. Robertson, K. Woje and T. A. Engh, Fluid Dynamics in Bubble Stirred Ladles: Part I. Experiments, *Metallurgical Transactions*, 19B (1988) 745-754.
[9] G. Montante, D. Horn and A. Paglianti. Gas-liquid flow and bubble size distribution in stirred tanks, *Chemical engineering science*, 63 (8) (2008) 2107-2118.
[10] L. Sirovich, Turbulence and The Dynamics of Coherent Structures PART I: Coherent Structures, *Quarterly of Applied Mathematics*, 45 (1987) 561-571.
[11] K. C. Kim, Y. U. Min, S. J. Oh, N. H. An, B. Seoudi, H. H. Chun and I. Lee, Time-Resolved PIV Investigation on the Unsteadiness of a Low Reynolds Number Confined Impinging Jet, *Journal of visualization*, 10 (4) (2007) 367-380.

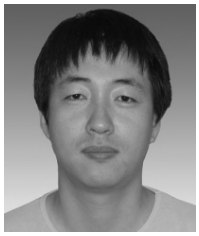

Hyun Dong Kim Ph.D. Candidate in the Department of Mechanical Engineering of Pusan National University He received the M.S. degree in Mechanical Engineering from Pusan National University in 2005. His main research interest is the development of fluid measurement techniques in the micro-scale such as micro-PIV, micro-LIF, and defocusing digital PTV. He is also interested in particle manipulation in a microchannel using a pneumatic micro-pump.

Seung Jae Yi, He received the B.S. degree in Mechanical Engineering from Pusan National University of Korea in 2007, and the M.S. degree in Mechanical Engineering from Pusan National University of Korea in 2009. His research interests are particle image velocimetry (PIV) measurement technology, characteristics of bio-fluids, and sensing chemistry using MEMS/NANO technology.

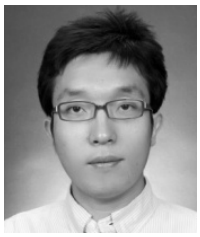

Jong Wook Kim, He received his B.S . (Eng) in Mechanical Engineering from KAIST (Korea Advanced Institute of Science and Technology), Korea in 1998, and his M.S degree in Mechanical Engineering from Hanyang University of Korea in 2000. He obtained his M.S degree with this paper's theme, experiment and analysis of counter-rotating axial fan. His research interests are measurement of thermal properties of thin film in nano scale using 3 omega method and thermal reflectance, and characteristics of flow by using POD (Proper Orthogonal Decomposition).

Kyung Chun Kim, Professor in the School of Mechanical Engineering of Pusan National University and Director of the MEMS/NANO Fabrication Center in Korea. He obtained the Ph.D. degree from the Korea Advanced Institute of Science and Technology (KAIST), Korea, in 1987. He was selected as a Member of the National Academy of Engineering of Korea in 2004. Since 2008, he has served as President of the Korean Society of Visualization. His research interests include 3D3C Micro-PIV, Bio-MEMS, micro/nanoscale energy transport, turbulence measurements based on PIV/LIF, micro-heat exchangers, biomechanics, biomedical engineering, POCT development for early detection of OP, wind turbines, and fuel cells.